Chemical Science

Accepted Manuscript

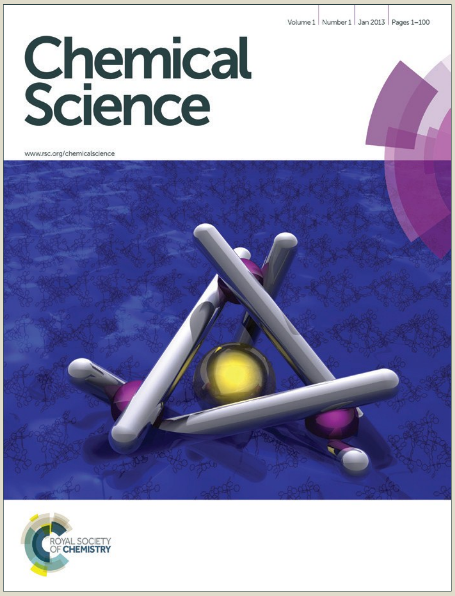

ROYAL SOCIETY OF CHEMISTRY

www.rsc.org/chemicalscience

A Noble Metal-Free Proton-Exchange Membrane Fuel Cell based on Bio-inspired Molecular Catalysts

P. D. Tran,[a#] A. Morozan,[b#] S. Archambault,[c#] J. Heidkamp,[d#] P. Chenevier,[e] H. Dau,[d] M. Fontecave,[af] A. Martinent,[c*] B. Jousselme,[b*] V. Artero[a*]

[a] *Laboratoire de Chimie et Biologie des Métaux ; Université Grenoble Alpes, CNRS, CEA; 17 rue des Martyrs, 38054 Grenoble cedex 09, France*
[b] *CEA Saclay, IRAMIS, NIMBE, UMR 368, Laboratory of Innovation in Surface Chemistry and Nanosciences (LICSEN), Gif sur Yvette F-91191, France.*
[c] *Institut LITEN CEA LITEN/DTNM/LCSN, Grenoble, France*
[d] *FB Physik, Free University Berlin, Berlin, Germany*
[e] *Université Grenoble Alpes, CNRS, CEA, INAC-SPRAM, F-38000 Grenoble, France*
[f] *Collège de* France, 11 place Marcelin Berthelot 75005 Paris, France.

[#] *these authors equally contributed to the work*

Abstract

Hydrogen is a promising energy vector for storing renewable energies: obtained from water-splitting, in electrolysers or photoelectrochemical cells, it can be turned back to electricity on demand in fuels-cells (FC). Proton exchange membrane (PEM) devices with low internal resistance, high compactness and stability is an attractive technology optimized over decades and affording fast starting and low operating temperature. However they rely on the powerful catalytic properties of noble metals such as platinum while lower cost, more abundant materials would be needed for economic viability. Replacing these noble metals at both electrodes has long proven to be a difficult task, so far incompatible with PEM technologies. Here we take advantage of newly developed bio-inspired molecular H_2 oxidation catalysts and noble-metal free O_2-reducing materials, to fabricate a noble metal-free PEMFC fuel cell, with 0.74 V open circuit voltage and 23 $\mu W \cdot cm^{-2}$ output power under technologically relevant conditions. X-ray absorption spectroscopy measurements confirm that the catalysts are stable and retain their structure during turnover.

Main text

Proton exchange membrane (PEM) technology currently stands as the most promising one for both portable and automotive applications. PEMFC have low internal resistance, high compactness and stability. After optimization over decades, they display high efficiency, start fast and operate at low temperature. However, they require platinum to catalyse both H_2 oxidation reaction (HOR) and O_2 reduction reaction (ORR) which hampers their economic viability and sustainability. Substituting earth-abundant catalysts for noble metals is thus critical. Significant progress has been achieved regarding the development of ORR catalysts[1-7] but no PEMFC using earth-abundant catalysts at both electrodes has been reported so far.

We recently reported on noble metal-free catalysts for HOR[8, 9] working under highly acidic conditions compatible with PEM technology. Hydrogenases[10, 11] are unique metalloproteins that catalyse HOR as efficiently as platinum nanoparticles do and in particular with remarkably high reaction rates (1500-9000 s^{-1} at pH 7 and 37°C in water).[12] Their active sites (Fig. 1) have inspired the design of new synthetic HOR catalysts, the most efficient ones being bisdiphosphine nickel complexes[13] exquisitely combining a nickel centre in an electron-rich environment as found in NiFe hydrogenases with proton relays provided by a pendant base mimicking the aza-propanedithiolato cofactor of FeFe hydrogenases.[14] In both classes of hydrogenases,[15] the presence of basic residues at the vicinity of the catalytic metal centre indeed facilitates the activation and heterolytic cleavage of H_2. Immobilization of such synthetic catalysts, either covalently or through π-π stacking interactions, on multiwall carbon nanotubes (CNTs) yielded Ni-CNT HOR catalytic nanomaterials. [8, 9] When interfaced with a Nafion membrane, these nanomaterials show catalytic activity for hydrogen evolution/uptake at the thermodynamic equilibrium, prolonged stability under turnover conditions and resistance to CO poisoning. It was thus tempting to implement these original materials as anode PEMFC catalyst. Here we report the first functional PEMFC based on earth-abundant materials at both anode and cathode.

Deposition of one of these Ni-CNT HOR materials on a Nafion membrane was first achieved through spray coating.[16] The preparation of a catalytic ink with suitable rheological properties required partial substitution of CNTs for carbon black nanoparticles with lower form factor. The anode Ni-CNT ink was then composed of $[Ni(P^{Ph}{}_2N^{CH_2pyrene}{}_2)_2](BF_4)_2$/CNTs (Ni-CNT, 30 wt. % dry mass) material (Fig. 1),[9] Vulcan XC-72 (40-50 wt. %) and Nafion (20-30 wt. %) in a water/isopropanol mixture (80/20 wt. %). The use of a 5:1 Vulcan XC-72:CNTs mass ratio led to particles in the 10-100 μm range as measured by dynamic light scattering.

A novel Co-N-C ORR catalyst with suitable rheological properties was obtained through adaptation of a previous procedure developed by some of us. [3,16] Pyrolysis of a mixture of a N-heterocyclic organic compound (triazolopyridine) and Vulcan XC-72 in the presence of $Co(NO_3)_2$ [3, 17] at 700 °C gave a fine dispersion of 0.1-100 μm particles in Nafion ((20-30 wt. %) water/isopropanol as a proper ink for spray coating. By analogy with the previously described material, the ORR activity is assigned to pyridinic-N functions located at the surface of the carbon matrix and binding cobalt ions as well as metallic cobalt nanoparticles.[3] This material displays overpotential for ORR ~300 mV higher than Pt/C in half cell configuration and good stability for more than 15h during chrono-amperometry measurements. A detailed structural and catalytic study is provided in the Supporting Information.

After spray coating of the catalytic inks (0.44 to $0.64 mg\cdot cm^{-2}$, corresponding to about 10 μm thickness) on both sides of a NRE-212 Nafion membrane ($5.76\ cm^2$) at 60-80 °C, the assembly was hot-pressed (50 °C, $2\cdot10^5$ Pa, 3 min) to improve catalyst-electrolyte contact and metal collectors were deposited on each side by evaporation of a gold layer, thin enough to allow for gas permeation. The resulting membrane-electrode assembly (MEA, Figure 2) was assessed at 60 °C in air under natural convection and ambient humidity in a dedicated micro fuel-cell test-rig. Partially humidified hydrogen ($20\ mL\cdot min^{-1}$ bubbling in water) was supplied to the anode, and air was passively supplied to the cathode.

The polarization and power density curves for the resulting Ni-CNT/Co-N-C PEMFC are shown on Fig. 2. Table 1 compares the performances of this noble metal-free PEMFC with other cells in which one electrode has been replaced by a standard Pt-based electrode similarly prepared from 40% Pt/C catalytic material. The noble metal-free PEMFC proved functional with an open-circuit voltage (OCV) of 0.74 V to be compared with the 1.0 V OCV value measured for a Pt/Pt PEMFC under the same conditions. The Ni-CNT/Pt and the Pt/Co-N-C control PEMFCs provided OCV values only 150 and 210 mV lower respectively than a standard Pt/Pt PEMFC, showing that each noble metal-free catalyst operates at reasonable overvoltages. The maximum power density of the noble metal-free PEMFC was $23\ \mu W\cdot cm^{-2}$ under dynamic conditions and stabilized at $20\ \mu W\cdot cm^{-2}$ under stationary conditions. From Table 1, it can be concluded that the ORR catalyst, tested against Pt in a full PEMFC device, shows a higher current density (13 mA.cm^{-2}) than in half-cell configuration (1—3 mA.cm^{-2}, Figures S4-S5) but the reverse is observed for the HOR catalyst (0.224 mA.cm^{-2} in PEMFC *versus* 1 mA.cm^{-2} in half-cell configuration, Figure S6). The limitation in terms of current density and output power thus comes here from the bio-inspired anode material and its interfacing with the membrane rather than from the cathode catalyst, indicating direction for further improvement of performances. Finally operation of Pt/Co-N-C and Ni-CNT/Pt PEMFCs at temperatures increasing from 25 °C to 60 °C showed a low increase in current density by a factor of ≤ 1.5, corresponding to an activation energy below 10 kJ·mol^{-1} and 20 kJ·mol^{-1}, respectively. These low activation energy values show that the current is likely limited by the gas transport processes in the bulk of the electrode materials.

We then performed X-ray absorption spectroscopy (XAS) measurements to identify the active species at work in the device. X-ray absorption spectra were realized directly on the MEA, before and after 1 hour continuous operation.

X-ray absorption near edge structure (XANES) and extended X-ray absorption fine structure (EXAFS) data recorded at the Co K edge on Co-N-C cathodes before and after O_2-reduction catalysis are presented in Fig. 3. The spectra exhibited two distinct contributions from metallic Co and a non-metallic ionic cobalt compound. Metallic cobalt is the major species in the as-prepared material but this contribution is lowered to 28±15 % of the total Co concentration after fuel cell operation. This oxidative transformation is not correlated to any loss of activity. Rather, it is consistent with the quite positive potential of the cathode during turnover in the contact with air. Comparison with the Co K edge positions of $[Co(H_2O)_6](NO_3)_2$ and $LiCoO_2$, containing Co^{II} and Co^{III} ions respectively, indicates an oxidation state between +II and +III for the cobalt ions in the catalytic material during operation while EXAFS analysis indicates coordination of cobalt ions to O or N atoms (Fig. S9). The Co-N-C material thus behave similarly to the cobalt-polypyrrole composite material previously reported by Bashyam and Zelenay.[2]

The as-prepared Ni-CNTs anode nanomaterial was compared with the molecular Ni catalyst (Fig. 4 and S10) to get insight into the molecular state of the metal catalytic centers. The presence of the sputtered gold electrode strongly reduced the quality of the XAS signal on the anode, so that we turned to previously described half-cell experiments with the Ni-CNT material deposited on a gas diffusion layer.[8, 9] As previously reported,[9] the Ni-edge EXAFS spectrum of Ni-CNTs before operation could be decomposed into the weighted addition of the spectra for pure molecular $[Ni(P^{Ph}_2N^{CH_2pyrene}_2)_2]$ catalyst and for Ni^{II} ions coordinated to lighter atoms as in $[Ni(H_2O)_6]^{2+}$, indicating that about $2/3^{rd}$ of the Ni complex remains in NiP_4 state (Table S2). After 1 hour operation for H_2 oxidation at 0.25 V vs RHE and in direct contact with 0.5 M aqueous H_2SO_4 electrolyte, the signal assigned to decomposed Ni complex disappears, leaving a pure NiP_4 signature (Fig 4, S10 and Table S2).[18] As the current density remains constant during the whole measurement (Fig. S4), corresponding to 4000 turnovers achieved for each NiP_4 species, we conclude that the decomposed Ni compound was washed off from the material during the electrochemical measurement. Additionally this experiment tells us that the bio-inspired NiP_4 complex is the only species responsible for catalysis and that it does withstand extensive PEM fuel cell operation with complete retention of its molecular structure.

We have thus successfully demonstrated the potential of the bio-inspired chemistry approach for the development of novel fuel-cells based exclusively on non-noble metals. Previously described Earth-abundant catalytic HOR and ORR materials have been assessed either in half-cell measurements or in combination with a platinum-based counter electrode material. Here, we report the first example of an operational PEMFC using a bio-inspired Ni-based material at the anode and a Co-based material at the cathode. Importantly, the operation and feeding conditions used in our study correspond to the expected daily use of market-dedicated micro devices and the performances reported here compare well with those of the first generation of H_2/O_2 enzymatic fuel cells.[19-21] Further improvements of the performances of the devices can be expected from optimization of ink formulation and control of the tridimensional structure of the electrodes as previously demonstrated for H_2/O_2[22-25] or glucose/O_2[26] biofuel cells.

anode	cathode	OCV *V*	I @ 0.2V $\mu A \cdot cm^{-2}$	P_{max} $\mu W \cdot cm^{-2}$
Pt	Co-N-C	0.79	1.310^4	2600

Ni-CNT	Pt	0.85	224	70
Ni-CNT	Co-N-C	0.74	94	23
Pt	Pt	1.00	$1.75\ 10^5$	$1.05\ 10^3$

Table 1. Open circuit voltage (OCV), current density and maximum power density generated by various PEMFC based on Ni-CNT, Co-N-C or Pt catalysts, PEMFC recorded at 60 °C with supply of partially humidified H_2 (20 mL·min^{-1}) at the anode and passive air convection at the cathode.

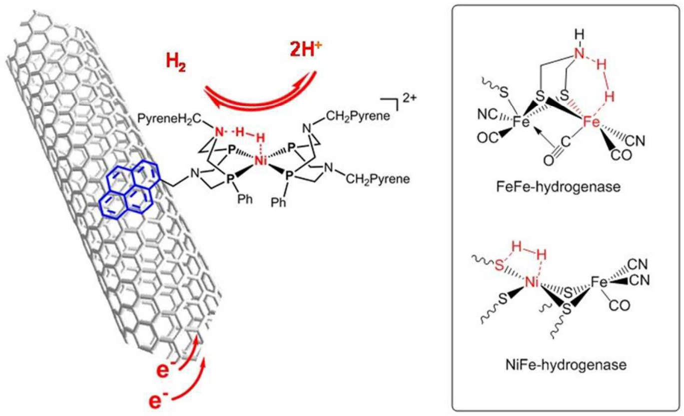

Figure 1. Structure of the Ni-CNT HOR catalyst based on a synthetic nickel bisdiphosphine complex inspired from the structures of the active sites of FeFe and NiFe hydrogenases shown in the inset.

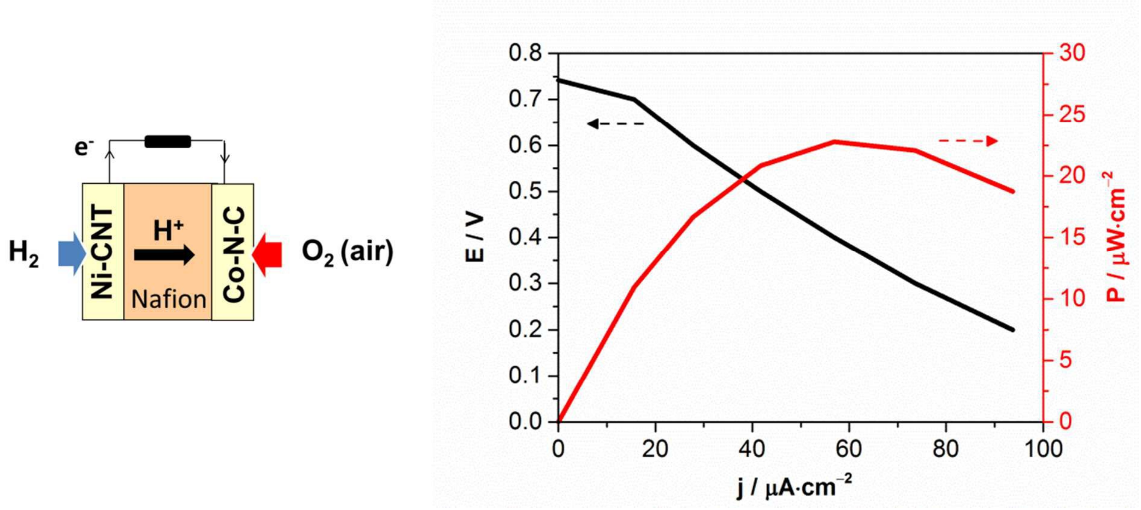

Figure 2. Left: Schematic description of the PEMFC assembly; right: Polarization and power density curves of the Ni-CNT/Co-N-C PEMFC recorded at 60 °C with supply of partially humidified H_2 (20 mL·min^{-1}) at the anode and passive air convection at the cathode.

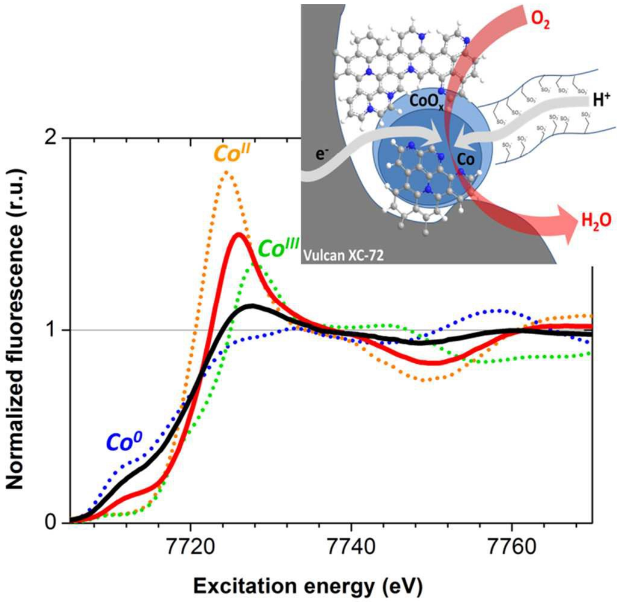

Figure 3. X-ray absorption near edge structure spectra (Co K edge) of Co-N-C material measured on the as-prepared material (black solid line) and after O_2-reduction catalytic operation (red solid line). The spectra of metallic Co (blue dotted line), $[Co^{II}(H_2O)_6](NO_3)_2$ (orange dotted line) and $LiCo^{III}O_2$ (green dotted trace) standards are also shown for comparison. Inset: representation of the Co-N-C material with carbon and nitrogen atoms depicted in grey and blue respectively.

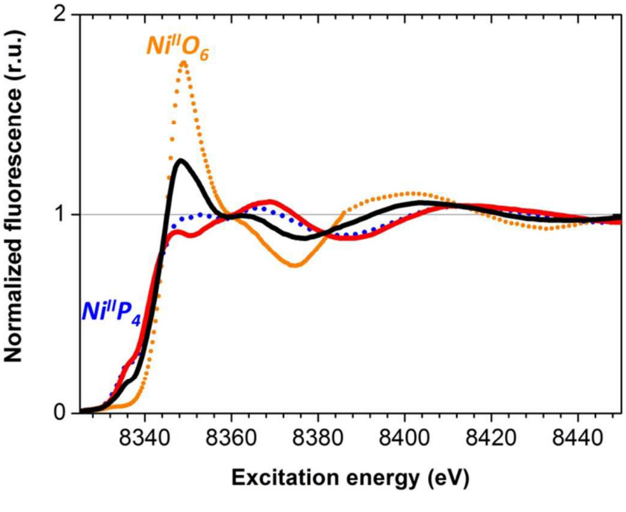

Figure 4. X-ray absorption near edge structure spectra (Ni K edge) of Ni-CNT as prepared (black solid line), and after 1h H_2 oxidation (red solid line). Spectra of pristine $[Ni(P^{Ph}{}_2N^{CH_2pyrene}{}_2)_2]$ (blue dotted line) and of $[Ni(OH_2)_6]^{2+}$ (orange dotted line) are shown for comparison. See Figure S10 for a magnification of the K edge region

Acknowledgements

This work was supported by ANR (EnzHyd project, ANR-08-PANH-008 and Labex program ARCANE, ANR-11-LABX-0003-01) and the FCH Joint Undertaking (Nano-Cat project, grant n° 325239). The XAS measurements were carried out at beamline KMC-1 of the BESSY synchrotron operated by the Helmholtz Zentrum Berlin (HZB); we thank M. Mertin and Dr. F. Schäfers (both HZB) for their technical support and the Berlin cluster of excellence on Unifying Concepts in Catalysis (UniCat) for the financial support.

References

1. M. Lefevre, E. Proietti, F. Jaouen and J. P. Dodelet, *Science*, 2009, **324**, 71-74.
2. R. Bashyam and P. Zelenay, *Nature*, 2006, **443**, 63-66.
3. A. Morozan, P. Jegou, B. Jousselme and S. Palacin, *Phys. Chem. Chem. Phys.*, 2011, **13**, 21600-21607.
4. K. P. Gong, F. Du, Z. H. Xia, M. Durstock and L. M. Dai, *Science*, 2009, **323**, 760-764.
5. R. Liu, D. Wu, X. Feng and K. Müllen, *Angew. Chem. Int. Ed.*, 2010, **49**, 2565-2569.
6. A. Morozan, B. Jousselme and S. Palacin, *Energy Environ. Sci.*, 2011, **4**, 1238-1254.
7. S. Pylypenko, S. Mukherjee, T. S. Olson and P. Atanassov, *Electrochim. Acta*, 2008, **53**, 7875-7883.
8. A. Le Goff, V. Artero, B. Jousselme, P. D. Tran, N. Guillet, R. Metaye, A. Fihri, S. Palacin and M. Fontecave, *Science*, 2009, **326**, 1384-1387.
9. P. D. Tran, A. Le Goff, J. Heidkamp, B. Jousselme, N. Guillet, S. Palacin, H. Dau, M. Fontecave and V. Artero, *Angew. Chem. Int. Ed.*, 2011, **50**, 1371-1374.
10. W. Lubitz, H. Ogata, O. Rüdiger and E. Reijerse, *Chem. Rev.*, 2014, **114**, 4081-4148.
11. P. Chenevier, L. Mugherli, S. Darbe, L. Darchy, S. DiManno, P. D. Tran, F. Valentino, M. Iannello, A. Volbeda, C. Cavazza and V. Artero, *C. R. Chim.*, 2013, **16**, 491-516.
12. A. K. Jones, E. Sillery, S. P. J. Albracht and F. A. Armstrong, *Chem. Commun.*, 2002, 866-867.
13. T. Ueno, M. Ohashi, M. Kono, K. Kondo, A. Suzuki, T. Yamane and Y. Watanabe, *Inorg. Chem.*, 2004, **43**, 2852-2858.
14. G. Berggren, A. Adamska, C. Lambertz, T. R. Simmons, J. Esselborn, M. Atta, S. Gambarelli, J. M. Mouesca, E. Reijerse, W. Lubitz, T. Happe, V. Artero and M. Fontecave, *Nature*, 2013, **499**, 66-69.
15. T. R. Simmons, G. Berggren, M. Bacchi, M. Fontecave and V. Artero, *Coord. Chem. Rev.*, 2014, **270–271**, 127-150.
16. Y. Matsubara, E. Fujita, M. D. Doherty, J. T. Muckerman and C. Creutz, *J. Am. Chem. Soc.*, 2012, **134**, 15743-15757.

17. A. Morozan, P. Jegou, M. Pinault, S. Campidelli, B. Jousselme and S. Palacin, *Chemsuschem*, 2012, **5**, 647-651.
18. The same behavior is observed if the material is simply equilibrated with the aqueous electrolyte during the measure of a few cyclic voltammograms or if the experiment is carried out during 1h under H2 evolution conditions (Fig. S11 and Table S2). If the same measurement is carried out on the Ni-CNTs material coated with a Nafion membrane, the XANES signal is unmodified even after 1 hour operation for H2 evolution at –0.3 V vs RHE.
19. K. A. Vincent, J. A. Cracknell, O. Lenz, I. Zebger, B. Friedrich and F. A. Armstrong, *Proc. Natl. Acad. Sci. USA*, 2005, **102**, 16951-16954.
20. K. A. Vincent, J. A. Cracknell, J. R. Clark, M. Ludwig, O. Lenz, B. Friedrich and F. A. Armstrong, *Chem. Commun.*, 2006, 5033-5035.
21. A. F. Wait, A. Parkin, G. M. Morley, L. dos Santos and F. A. Armstrong, *J. Phys. Chem. C*, 2010, **114**, 12003-12009.
22. L. Xu and F. A. Armstrong, *Energy Environ. Sci.*, 2013.
23. S. Krishnan and F. A. Armstrong, *Chem. Sci.*, 2012, **3**, 1015-1023.
24. A. Ciaccafava, A. De Poulpiquet, V. Techer, M. T. Giudici-Orticoni, S. Tingry, C. Innocent and E. Lojou, *Electrochem. Commun.*, 2012, **23**, 25-28.
25. A. de Poulpiquet, H. Marques-Knopf, V. Wernert, M. T. Giudici-Orticoni, R. Gadiou and E. Lojou, *Phys. Chem. Chem. Phys.*, 2014, **16**, 1366-1378.
26. A. Zebda, C. Gondran, A. Le Goff, M. Holzinger, P. Cinquin and S. Cosnier, *Nat. Commun.*, 2011, **2**, 370.